

Scattering on dislocations and cosmic strings in the geometric theory of defects

M. O. Katanaev* and I. V. Volovich†

*Steklov Mathematical Institute,
Gubkin St., 8, Moscow, 117966, Russia*

12 May 1998

Abstract

We consider scattering of elastic waves on parallel wedge dislocations in the geometric theory of defects or, equivalently, scattering of point particles and light rays on cosmic strings. Dislocations are described as torsion singularities located on parallel lines, and trajectories of phonons are assumed to be the corresponding extremals. Extremals are found for arbitrary distribution of the dislocations in the monopole, dipole, and quadrupole approximation and the scattering angle is obtained. Examples of continuous distribution of wedge and edge dislocations are considered. We have found that for deficit angles close to -2π a star located behind a cosmic string may have any even number of images, 2, 4, 6, . . . The close relationship between dislocations and conformal maps is elucidated in detail.

*E-mail: katanaev@mi.ras.ru

†E-mail: volovich@mi.ras.ru

1 Introduction

Geometric description of defects in solids has attracted continuous interest in the last years. The central role here is played by torsion. This geometric notion was introduced by E. Cartan [1] (see also [2]) and, quite interesting, by analogy with elastic media. Later the relation of torsion to dislocations was noticed [3, 4] (see reviews [5-7]), and disclinations in spin glasses or liquid crystals were found to correspond to nontrivial curvature of a $SO(3)$ -connection [8]. Elastic media with a spin structure (Cosserat media [9]) containing arbitrary distribution of dislocations and disclinations can be consistently described in the framework of general Riemann–Cartan geometry where torsion and curvature are identified with surface densities of Burgers and Frank vectors, respectively [10] (a similar approach was discussed in [11]). Generalizations of gravity models to Riemann–Cartan and general affine geometry are reviewed in [12]. It should be stressed that geometric description treats single as well as continuously distributed defects in a unified manner.

The advantage of geometric description of defects in solids is twofold. First, in contrast to the ordinary elasticity theory this approach provides an adequate language for continuous distribution of defects. Second, a mighty mathematical machinery of differential geometry clarifies and simplifies calculations.

From a mathematical point of view geometric theory of defects in solids and the theory of gravity with torsion in the Euclidean formulation are the same models. The relation between N point particle solution of three dimensional gravity [13–15] and wedge dislocations was first analyzed in [16, 17]¹. (See also [18, 19].) In [10] we proposed a three dimensional action for describing defects in solids and showed that description of an arbitrary distribution of static parallel dislocations naturally arises from an action principle. This solution defines nontrivial geometry on R^3 manifold of zero curvature with N removed parallel lines corresponding to torsion singularities. Each of the removed lines defines a conical singularity in the perpendicular plane. In spite of the fact that the curvature is zero the whole space is not a manifold with absolute parallelism because parallel transport of a vector around conical defect produces rotation on a deficit angle. A gauge approach to the theory of defects in solids and cosmic strings is adopted in [20]. Recently a series of articles dealing with the physical properties of the N point particle solution appeared [21–26].

In the present paper we analyze scattering of elastic waves on parallel wedge dislocations. In the eikonal approximation or geometric optics [27] elastic deformations described by the wave equation move along extremals. By analogy with motion of photons in electrodynamics it is natural to assume that extremals are trajectories of phonons in elastic media with defects². In this way analysis of extremals yields a complete picture of the scattering of phonons on dislocations. In the case under

¹There wedge dislocations are called disclinations. The last name is also used in describing defects in a spin structure of a media. The geometric theory describes both types of defects, and therefore we reserve the name disclination for a defect in a spin structure.

²An alternative point of view is adopted in [28] where a point particle is assumed to move along geodesic (there extremals and geodesics are called geodesics and autoparallels, respectively).

consideration the scattering problem is not the standard one because in general the space is not asymptotically flat. For example, the notion of a falling beam of parallel moving particles depends on the distance to the dislocation, and the standard definition of a cross section does not work. At the same time one can easily define the scattering angle considering asymptotics of a particle trajectory. For one wedge dislocation we derive the following scattering angle

$$\chi = \frac{\pi\theta}{1+\theta}, \quad (1)$$

where $2\pi\theta$ is the deficit angle that is the angle of the wedge which is removed ($-1 < \theta < 0$) or added ($0 < \theta$) to the media.

Extremals for one edge dislocation were analyzed perturbatively in [24]. Recently extremals were analysed for one dispiration defect containing a wedge dislocation as a special case [25]. In the present paper we extend these results and analyze extremals nonperturbatively for arbitrary distribution of wedge parallel dislocations. In fact, a general explicit expression for an extremal is obtained. Already for one wedge dislocation we obtain a very rich and interesting scattering picture of phonons. In particular, if the deficit angle is close to -2π or $\theta \approx -1$ then a phonon makes several turns around the dislocation before going to infinity. If dislocations are more concentrated in a compact domain of the perpendicular plain than at large distances one may use perturbation theory. In this way we analyzed monopole, dipole, and quadrupole contributions. The dipole approximation coincides with the scattering on an edge dislocation.

The spatial part of the metric for a static cosmic string [29, 30] coincides with the metric for a wedge dislocation although it was obtained in a quite different manner by solving four dimensional Einstein equations for a cosmic string in the linear approximation. Therefore scattering of elastic waves on dislocations is the same as scattering of point particles or photons on cosmic strings. We derive a general formula for the angular separation between images of a star located behind a cosmic string. For small angles the expression coincides with the result obtained earlier, and there are only two images. If the deficit angle approaches -2π then the number of images increases because an observer sees the light rays which make no rotation around the string, one rotation, two rotations, and so on.

The results are applicable to a radial disgyration defect in ${}^3\text{He-A}$, described by a conical singularity, too [31].

In Section 2, a general framework for the analysis of extremals is briefly described. It is applied to extremals in the case of one wedge dislocation in Section 3. In Section 4 we calculate the angular separation between the images of a star located behind a cosmic string. The analysis of extremals is extended to arbitrary distribution of wedge dislocations in Section 5. In Section 6 we show that parallel linear dislocations are described by the conformal map of the Christoffel-Schwarz type. The dipole approximation corresponding to pure edge dislocation is considered in detail in Section 7. In Section 8 we study the quadrupole approximation. Two simple examples of continuous distribution of dislocations are considered in Section 9.

2 A general framework

We suppose that elastic media with dislocations is an R^3 manifold with some punctures and/or removed lines corresponding to the cores of dislocations and a given Riemann–Cartan geometry [10]. An arbitrary curvilinear coordinate system is denoted by x^μ , $\mu = 1, 2, 3$. A Riemann–Cartan geometry is defined by metric and torsion or, equivalently, by triad and $SO(3)$ -connection. Here we use the more convenient second set of variables called Cartan variables. Pure dislocations correspond to zero curvature

$$R_{\mu\nu}{}^{ij} = \partial_\mu \omega_\nu{}^{ij} - \omega_\mu{}^{ik} \omega_{\nu k}{}^j - (\mu \leftrightarrow \nu) = 0, \quad (2)$$

but nontrivial torsion. Here $\omega_\mu{}^{ij} = -\omega_\mu{}^{ji}$, $i, j, \dots = 1, 2, 3$, is an $SO(3)$ -connection considered as an independent variable. For zero curvature it is a pure gauge and can be always set to zero at least locally by means of local $SO(3)$ rotation. This can be done in domains with the trivial fundamental group which are spaces with absolute parallelism. If the space contains singularities and one has to remove infinite or closed lines from R^3 then this property is violated but may be restored by making appropriate cuts. A triad field $e_\mu{}^i$ defines a metric $g_{\mu\nu}$ in the usual way

$$g_{\mu\nu} = e_\mu{}^i e_\nu{}^j \delta_{ij}, \quad \delta_{ij} = \text{diag}(+++). \quad (3)$$

In our case torsion tensor,

$$T_{\mu\nu}{}^i = \partial_\mu e_\nu{}^i - \omega_\mu{}^{ij} e_{\nu j} - (\mu \leftrightarrow \nu),$$

is entirely defined by the triad because the $SO(3)$ -connection is set to zero.

Of course, for a given metric (3) one can construct Christoffel's symbols and the corresponding curvature as if torsion equals zero. It will be not the same curvature as given by (2) and is nontrivial in the presence of dislocations.

We assume that phonons in the media with dislocations move along extremals defined by the metric (3). Extremals $x^\mu(t)$ satisfy the well known set of equations

$$\ddot{x}^\mu = -\Gamma_{\nu\rho}{}^\mu \dot{x}^\nu \dot{x}^\rho, \quad (4)$$

where $\Gamma_{\nu\rho}{}^\mu$ denotes Christoffel's symbols (the Levi–Civita connection) constructed from the metric (3). Note that extremals coincide with geodesics in Riemann–Cartan geometry if and only if torsion is zero or antisymmetric in all three indices. In three dimensions the canonical parameter t is interpreted as the time. Indeed, extending three-dimensional space to four-dimensional space-time, $x^\mu \rightarrow (x^0, x^\mu)$, and assuming the following form of the four-dimensional metric

$$\begin{pmatrix} -1 & 0 \\ 0 & g_{\mu\nu} \end{pmatrix},$$

one finds the fourth equation for an extremal

$$\ddot{x}^0 = 0 \quad \Leftrightarrow \quad \dot{x}^0 = at + b, \quad a, b = \text{const.}$$

Thus up to a linear transformation the canonical parameter coincides with the real time x^0 .

Analysis of extremals becomes simpler if one notices that there is always one integral to equations (4)

$$g_{\mu\nu}\dot{x}^\mu\dot{x}^\nu = C_0 = \text{const} > 0, \quad (5)$$

which means that the length of the tangent vector or the square of the velocity of a phonon (the kinetic energy) remains constant. Another simplification occurs if the metric admits a Killing vector field k^μ ,

$$\nabla_\mu k_\nu + \nabla_\nu k_\mu = 0,$$

where ∇_μ denotes the covariant derivative with respect to Christoffel's symbols. In this case there exists another integral

$$g_{\mu\nu}k^\mu\dot{x}^\nu = C_1 = \text{const}, \quad (6)$$

which is related to the symmetry of the space. In two dimensions the existence of one Killing vector field is enough for the complete analysis of extremals because one has two integrals (5), (6) for two unknown functions. In higher dimensions complete analysis requires the existence of more Killing directions or some other techniques. The latter is also required in two dimensions in the absence of a Killing vector field.

Another approach to the analysis of extremals is provided by the action principle. It is well known that equations (4) follow from the Lagrangian

$$L = \frac{1}{2}g_{\mu\nu}\dot{x}^\mu\dot{x}^\nu, \quad (7)$$

which equals the kinetic energy of a point particle of unit mass moving in a space with nontrivial geometry. Of course, here the canonical parameter and real time are naturally identified. We see that both phonons and point particles move along the same trajectories. The difference is only in the velocity of movement. If a particle carries charge or spin which directly interacts with the media then one has to add a potential term to the Lagrangian (7). In that case a trajectory will differ from an extremal. Although the potential term in (7) is absent the motion of a particle is nontrivial because the metric explicitly depends on a position. Then equations (4) are nothing more than the Newton law with the force quadratic in the velocity. Due to this circumstance the motion of phonons in the presence of a dislocation differs drastically from the Newtonian motion of a point particle in a potential field. For example, we shall find later a new type of closed trajectories.

If there is not enough symmetry for the complete analysis of extremals then the Hamilton–Jacobi equation may be useful. The Lagrangian (7) gives rise to the Hamiltonian

$$H = \frac{1}{2}g^{\mu\nu}p_\mu p_\nu,$$

where $g^{\mu\nu}$ is the inverse metric and $p_\mu = \partial L / \partial \dot{x}^\mu$ is the canonical momenta. Then the Hamilton–Jacobi equation for the characteristic function $S(x^\mu, t)$ takes the form

$$\frac{\partial S}{\partial t} + \frac{1}{2} g^{\mu\nu} \frac{\partial S}{\partial x^\mu} \frac{\partial S}{\partial x^\nu} = 0, \quad (8)$$

or

$$S(x^\mu, t) = W(x^\mu) - Et, \quad E = \text{const},$$

where

$$\frac{1}{2} g^{\mu\nu} \frac{\partial W}{\partial x^\mu} \frac{\partial W}{\partial x^\nu} = E. \quad (9)$$

Here E denotes the total (in our case kinetic) energy of a phonon. This equation is solved in Section 5 for arbitrary distribution of N wedge dislocations characterized by one Killing direction.

3 Extremals for a wedge dislocation

Let us analyze extremals in the simplest case of the media with one wedge dislocation, characterized by the deficit angle θ normalized on 2π , so that the real angle is equal to $2\pi\theta$ (see Fig.1). In this section we derive the formula (1) for the scattering angle. The x^3 axis is chosen along the core of dislocation. The corresponding metric

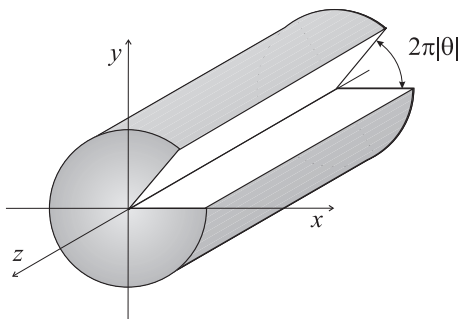


Figure 1: A wedge dislocation with the deficit angle $2\pi\theta$. For negative θ , $-1 < \theta < 0$, the wedge is removed from the media.

has the form [10]

$$ds^2 = dl^2 + (dx^3)^2, \quad (10)$$

where the nontrivial two-dimensional part of the metric in polar coordinates reads

$$dl^2 = r^{2\theta} (dr^2 + r^2 d\varphi^2). \quad (11)$$

This is the well known form of the metric for a conical singularity with the deficit angle $2\pi\theta$. It is not asymptotically flat, and particles at infinity cannot be considered

as free. They feel a wedge dislocation even at infinite distance. Christoffel's symbols corresponding to the metric (11) are easily calculated,

$$\begin{aligned}\Gamma_{rr}^r &= \frac{\theta}{r}, \\ \Gamma_{\varphi\varphi}^r &= -(1+\theta)r, \\ \Gamma_{r\varphi}^\varphi = \Gamma_{\varphi r}^\varphi &= \frac{1+\theta}{r},\end{aligned}$$

the others being identically zero. Then equations for an extremal (4) reduce to

$$\ddot{r} = -\frac{\theta}{r}\dot{r}^2 + (1+\theta)r\dot{\varphi}^2, \quad (12)$$

$$\ddot{\varphi} = -2\frac{1+\theta}{r}\dot{r}\dot{\varphi}, \quad (13)$$

$$\ddot{x}^3 = 0. \quad (14)$$

The last equation is the consequence of the translational symmetry along the x^3 axis, and shows that phonons move along it with a constant velocity. Therefore the scattering reduces to the two-dimensional problem in the r, φ plane. The metric for a wedge dislocation possesses a rotational symmetry around the x^3 axis. The corresponding Killing vector field in polar coordinates has a simple form

$$k^\mu = \begin{pmatrix} 0 \\ 1 \end{pmatrix}.$$

Thus integrals (5) and (6) for a wedge dislocation reduce to

$$r^{2\theta}\dot{r}^2 + r^{2(1+\theta)}\dot{\varphi}^2 = C_0 > 0, \quad (15)$$

$$r^{2(1+\theta)}\dot{\varphi} = C_1. \quad (16)$$

They have direct physical interpretation to be discussed later. For nonradial motion one easily finds the general form of an extremal

$$\left(\frac{r}{r_m}\right)^{2(1+\theta)} \sin^2[(1+\theta)(\varphi + \varphi_0)] = 1, \quad (17)$$

where

$$r_m = \left(\frac{C_1^2}{C_0}\right)^{\frac{1}{2(1+\theta)}}, \quad \varphi_0 = \text{const.} \quad (18)$$

We see that the form of an extremal is parametrized by two arbitrary constants. The constant r_m is positive and defines the length scale, while the constant φ_0 corresponds to rotational symmetry around the core of dislocation and may be arbitrary. Formula (17) describes an infinite number of disconnected branches depending on the range of the angle. One branch corresponds to the variation of the sin argument from $n\pi$ to $(n+1)\pi$, $|n| = 0, 1, \dots$. The radius is bounded from below $r_m < r < \infty$,

and every branch starts and ends at infinity. For $n = 0$ the angle $\varphi + \varphi_0$ varies from 0 to $\pi/(1 + \theta)$. For positive θ the variation of the angle is less than π , and a phonon is repelled from the dislocation. For negative θ phonons are attracted, and can make several turns around the dislocation. Suppose the extremal makes exactly m rotations. Then the angle $\varphi + \varphi_0$ varies from 0 to $2\pi m$, and the corresponding deficit angle θ_m is defined by the equation

$$(\theta_m + 1)2\pi m = \pi.$$

Extremals for a wedge dislocation are drawn in Figs.2–5 for different values of θ and $\varphi_0 = \pi$ ³. In the case $\theta > 0$ the extra wedge of media of angle $2\pi\theta$ is added to the media. For positive θ every extremal has two asymptotes going through the

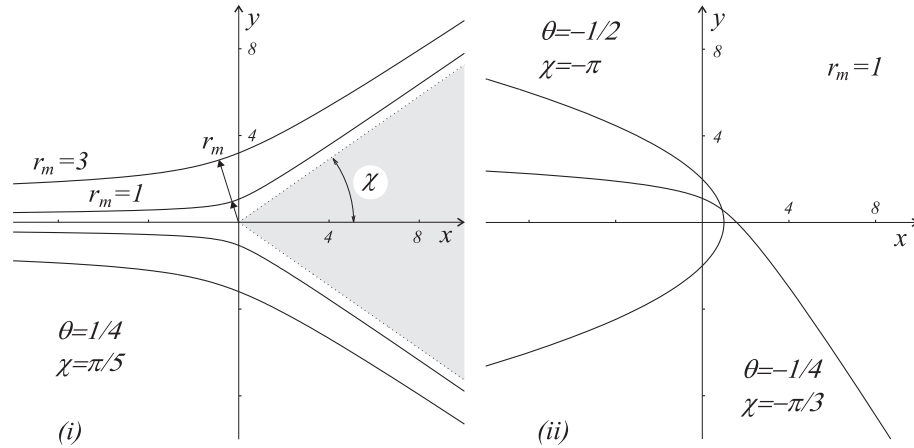


Figure 2: Extremals for a wedge dislocation with $\theta > 0$ (i) and $-1/2 \leq \theta < 0$ (ii). In (i) we draw two extremals and their reflections for the same θ but different r_m . In (ii) we draw two extremals for the same r_m but different θ . For $\theta = -1/2$ an extremal makes one turn around the dislocation.

center and intersecting at the scattering angle χ (see Fig.2(i)). The scattering angle is equal to $\pi - \Delta\varphi$ where $\Delta\varphi$ is the angle between two asymptotes for an extremal defined by equation (17), $(1 + \theta)\Delta\varphi = \pi$. In this way one immediately gets the expression

$$\chi = \pi - \frac{\pi}{1 + \theta} = \frac{\pi\theta}{1 + \theta}$$

which coincides with (1). The scattering angle has clear geometric interpretation. It equals one half of the deficit angle times the compression coefficient

$$\chi = \frac{2\pi\theta}{2} \times \frac{1}{1 + \theta}.$$

³All extremals in this and the following sections are drawn numerically, and the scale is shown in the drawings.

It means that the wedge dislocation is made by addition of uncompressed media and afterwards the media compresses. If one added the compressed wedge of the media then the compression coefficient would be absent. If θ goes to infinity then any extremal returns back from the dislocation along the same line. If the dislocation is absent, $\theta = 0$, then there is no scattering and $\chi = 0$. It is quite interesting that for positive θ there are points which cannot be joined by an extremal. For example, a point on the negative half of the x -axis cannot be joined by an extremal with arbitrary point lying in the wedge of inserted media (the shaded region in Fig.2(i)). The reason for this is the conical singularity at the origin of coordinate system.

For negative θ the wedge is removed from the media. In this case extremals have no asymptotes, but the scattering angle is still defined by the equation (1). In Fig. 2 (ii) we show two extremals for different θ but the same $r_m = 1$ which have up to one turn around the dislocation, one turn corresponding to $\theta = -1/2$ when half of the media is removed. If $-1 < \theta < -1/2$ then the phonon makes several turns around the dislocation before going to infinity as shown in Figs. 3-5. This kind

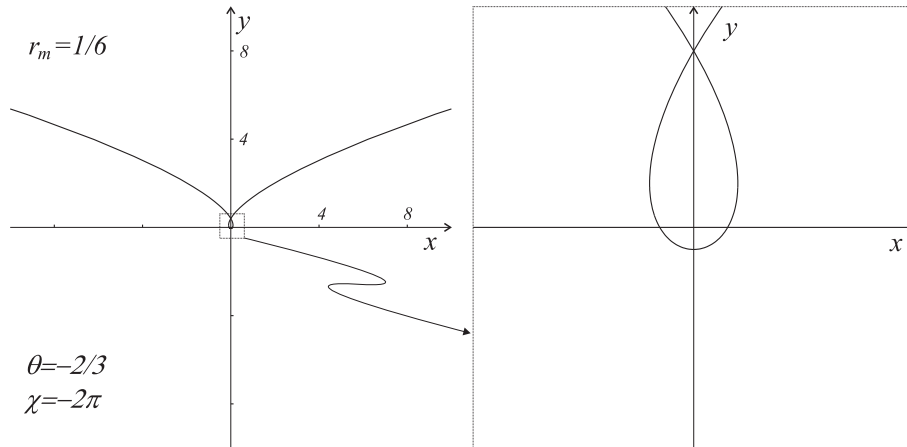


Figure 3: An extremal for $\theta = -2/3$ makes one turn around the dislocation and then goes forward in the same direction.

of trajectories is not specific only to the dislocations. Similar extremals are met already in the Schwarzschild space-time [32]. These trajectories produce multiple images of a star located behind the singularity.

At infinity $r \rightarrow \infty$ equations (15), (16) yield

$$\frac{1}{1+\theta} r^{1+\theta} = \sqrt{C_0 t} + const. \quad (19)$$

It means that for $\theta > -1$, a particle moves to space infinity in infinitely long time, and the manifold is complete at $r \rightarrow \infty$ (any extremal can be continued to infinite value of the canonical parameter in both directions). Later we show that the radial extremals can be continued through the singularity and become complete too. In

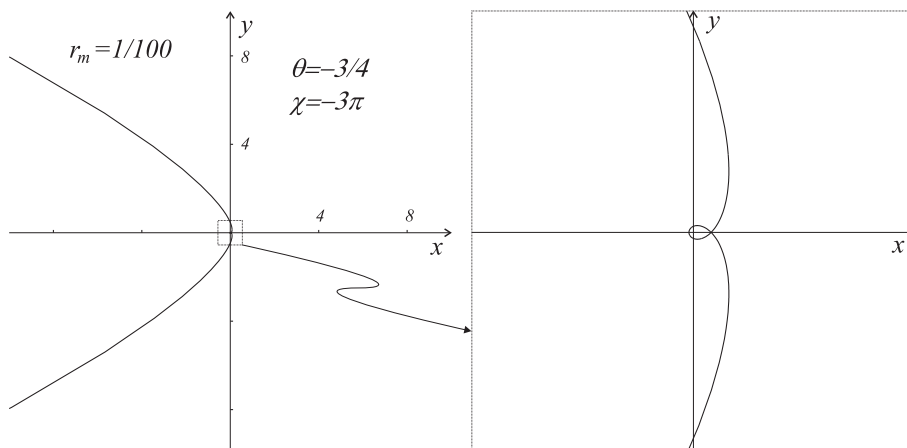


Figure 4: An extremal for $\theta = -3/4$ makes two turns around the wedge dislocation.

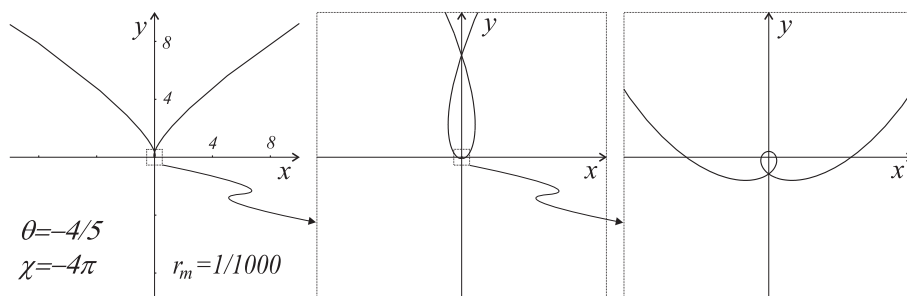


Figure 5: An extremal for $\theta = -4/5$ makes two turns and a half around the wedge dislocation before going to infinity.

this sense the whole manifold is complete. Unphysical region $\theta \leq -1$ corresponding to the case when one removes more than the whole media leads to an incomplete manifold which should be extended.

Physical interpretation of the first integrals (15), (16) is clear from the following consideration. In the primed coordinate system,

$$r' = \frac{1}{1+\theta} r^{1+\theta}, \quad \varphi' = (1+\theta)\varphi,$$

the line element (11) becomes flat

$$dl^2 = dr'^2 + r'^2 d\varphi'^2.$$

This means that in these coordinates phonons move along straight lines, and the energy, momentum, and angular momentum are conserved. The kinetic energy of a

phonon of unit mass is easily calculated

$$E' = \frac{1}{2}(\dot{r}'^2 + r'^2\dot{\varphi}'^2) = \frac{1}{2}C_0.$$

So the first integral (15) is proportional to the kinetic energy or the square of the velocity. The momentum is defined by C_0 and the direction of the trajectory. The calculation of the angular momentum,

$$L' = r'^2\dot{\varphi}' = \frac{1}{1+\theta}C_1,$$

yields physical interpretation for the other integration constant. It is defined by the initial condition of the system and is arbitrary. The constant of motion C_0 exists for the wave equation of acoustic waves [27] and is different for longitudinal and transverse phonons. This is the constant distinguishing trajectories of different waves. One may assume that point particles also move along extremals if they do not carry charge or spin which directly interact with the media. Then the constant C_0 is parametrizing the type of a phonon and a point particle. For a point particle it is defined by the initial condition and may be arbitrary. The form of an extremal (17) is defined by the constant (18) depending both on C_0 and C_1 . The constant C_1 is arbitrary and therefore phonons and point particles move along the same trajectories, the only difference being the velocity of movement.

Suppose that the external observer examines the scattering using some device which does not interact with the media. Then he observes the scattering on dislocation in polar coordinates r, φ which are flat for his device. For him the existence of dislocation exhibits itself as the bending of phonon trajectories.

Let us compute physical characteristics of the scattering phonon as measured by an external observer for whom a dislocation appears through the properties of a phonon. The observed kinetic energy,

$$E = \frac{1}{2}(\dot{r}^2 + r^2\dot{\varphi}^2) = \frac{1}{2}C_0r^{-2\theta}, \quad (20)$$

is positive and explicitly depends on the distance to the dislocation. It decreases and increases for positive and negative deficit angle θ , respectively, as the phonon approaches the dislocation. At the infinity the energy tends to zero for positive θ and to infinity for negative θ :

$$\begin{aligned} \theta > 0 : \quad E &\rightarrow 0, \quad r \rightarrow \infty, \\ \theta < 0 : \quad E &\rightarrow \infty, \quad r \rightarrow \infty. \end{aligned}$$

Of course in a real world the energy cannot increase to infinity and is bounded by the finite size of the bodies. The radial and angular components on the momentum have the form

$$p_r = \dot{r} = \sqrt{C_0}r^{-2\theta-1}\sqrt{r^{2(1+\theta)} - r_m^{2(1+\theta)}}, \quad (21)$$

$$p_\varphi = r\dot{\varphi} = C_1r^{-2\theta-1}. \quad (22)$$

The absolute value of the angular component increases and decreases as the phonon goes closer to the dislocation for $\theta > -1/2$ and $-1 < \theta < -1/2$, respectively. For $\theta = -1/2$ it does not depend on the distance. The behavior of the absolute value of the radial component is more complicated. For $-1 < \theta < 0$ it grows up monotonically from zero to infinity as the radius grows from r_m to ∞ . For $\theta > 0$ it is zero both at r_m and infinity and has one maximum at

$$r = r_m \left(\frac{1 + 2\theta}{2\theta} \right)^{\frac{1}{2(1+\theta)}}.$$

The angular momentum as measured by an external observer,

$$L = r^2 \dot{\varphi} = C_1 r^{-2\theta},$$

also depends on the distance.

Radial extremals must be treated separately. Equation (16) for $\varphi = \text{const}$ and $C_1 = 0$ is satisfied, and equation (16) can be easily integrated

$$r^{1+\theta} = \sqrt{C_0}(1+\theta)(t+t_0), \quad t_0 = \text{const}.$$

For any deficit angle the core of dislocation is reached by the radial extremal at finite time. It is naturally continued through the conical singularity: we consider two radial extremals with angles φ and $\varphi+\pi$ as two halves of one complete extremal. This is one possibility when the phonon is considered to go through the conical singularity. The other possibility is to assume that the phonon reaches the singularity in finite time and disappears. The present model does not allow to choose between the alternatives, and one has to invoke other theoretical or experimental arguments. This is beyond the scope of the paper.

Note that circle extremals, $r = \text{const}$, are absent as the consequence of equation (12), though integrals (15), (16) admit this solution. This happens because to obtain the first integrals equations (12), (13) must be multiplied by \dot{r} .

The analysis of extremals shows that the motion of phonons is not a potential one. That is, there is no effective potential yielding the same trajectories in the flat Euclidean space. Indeed, the observed kinetic energy (20) suggests the potential

$$U = -\frac{1}{2}C_0 r^{-2\theta} + \text{const}$$

for the total energy to be conserved. Then one gets the Lagrangian

$$L = \frac{1}{2}\dot{r}^2 + \frac{1}{2}r^2\dot{\varphi}^2 + \frac{1}{2}C_0 r^{-2\theta}$$

with Euclidean metric but nontrivial potential. This Lagrangian yields qualitatively different trajectories for a particle.

4 Cosmic strings and multiple images

The metric for a wedge dislocation with a negative deficit angle, $\theta < 0$, coincides with the spatial part of the metric for a cosmic string first found in [33]. It is interesting that the metric for a cosmic string was obtained in a quite different way by solving four-dimensional Einstein equations in the linear approximation. Nevertheless the metric is essentially the same, and therefore extremals found in the previous section describe also light rays in the presence of a cosmic string. The well known effect of a cosmic string is the appearance of double images of a star located behind the cosmic string, see Fig. 6(i). In this section we derive a general formula for the angular

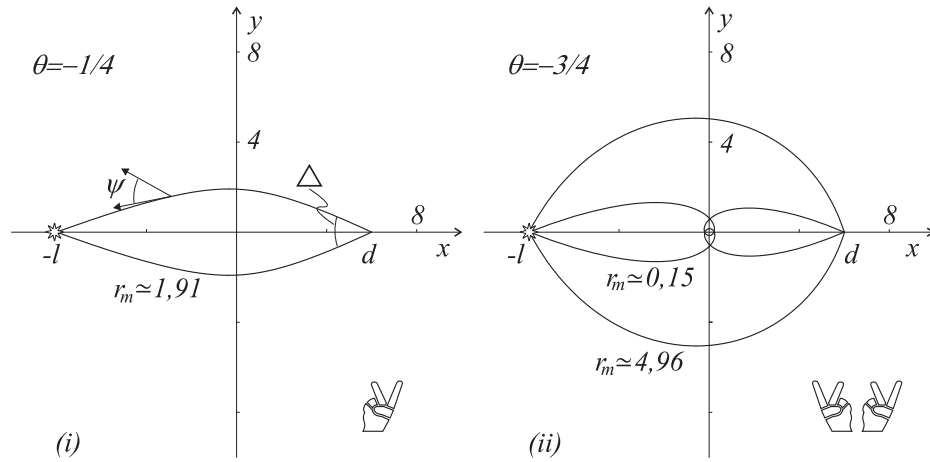


Figure 6: Double images of a star located behind a cosmic string with small deficit angle (i). If a deficit angle is close to -2π then a star may have any even number of images. In Fig. (ii) we show a star with four images, two of them being produced by light rays making one turn around a cosmic string.

separation between the images. Originally, the angular separation was obtained for small angles by calculating the angle in the coordinate system where extremals are straight lines (that is, in the media with removed wedge but not deformed). We obtain the formula which is valid for all angles and in the coordinate system describing the media after the dislocation is created.

Suppose that a star and an observer are located at distances l and d , respectively, as shown in Fig. 6. The angle ψ between the tangent vector to a light ray and the radial direction is defined by the expression

$$\tan \psi = \frac{rd\varphi}{dr}.$$

Using equation (17) one easily finds

$$\psi = -(1 + \theta)(\phi + \phi_0),$$

up to an addition of $2\pi n$, $|n| = 1, 2, \dots$. Location points of a star and observer are defined by the equation

$$\left(\frac{l}{r_m}\right)^{2(1+\theta)} \sin^2 \psi_1 = 1, \quad (23)$$

$$\left(\frac{d}{r_m}\right)^{2(1+\theta)} \sin^2 \psi_2 = 1, \quad (24)$$

where

$$\psi_1 = -(1+\theta)(\pi + 2m\pi + \varphi_0), \quad (25)$$

$$\psi_2 = -(1+\theta)\varphi_0. \quad (26)$$

Here m is the number of rotations of the light ray around the cosmic string before reaching the observer. The whole number of rotations of the corresponding extremal may be greater. The difference between ψ_2 and ψ_1 must be less than π . Otherwise a star and an observer would be crossed by different branches of an extremal. Therefore the inequality

$$(1+\theta)\pi(1+2m) < \pi \quad (27)$$

restricts the maximal number of rotations for a given deficit angle. As the consequence of equations (25) and (26) we have

$$\psi_2 = \psi_1 + \pi(1+\theta)(1+2m).$$

Denoting the angular separation between images by $\Delta = 2(\pi - \psi_2)$ one easily deduces from (23), (24) a general formula for the angular separation between two symmetric images produced by the light rays making m rotations around the string

$$d^{(1+\theta)} \left| \sin \frac{\Delta}{2} \right| = l^{(1+\theta)} \left| \sin \left(\frac{\Delta}{2} + \pi(1+\theta)(1+2m) \right) \right|. \quad (28)$$

Here m is any natural number satisfying the inequality (27). For small deficit angle, $|\theta| \ll 1$, an extremal cannot make a turn around the dislocation, $m = 0$. Therefore there are only two images separated by a small angle, $\Delta \ll 1$. In this case equation (28) reduces to the well known formula [29]

$$\Delta = \frac{l}{d+l} |2\pi\theta|. \quad (29)$$

The coincidence of the results is not trivial, because the angle is computed in different coordinate systems. It means that the coordinate transformation describing a defect creation must be described by a conformal transformation which preserves angles. This is indeed the case as will be shown in the next sections. In fact, this assumption was made but not written in the original derivation of (29).

Let us consider a general case (28) in more detail. Light rays emitted by a star are parametrized by the angle ψ_1 . They cross the x axis at point d defined by the equation

$$\left(\frac{d}{l}\right)^{2(1+\theta)} \frac{\sin^2[\psi_1 + (1+\theta)\pi(1+2m)]}{\sin^2 \psi_1} = 1. \quad (30)$$

We see that for a given m the observer at any distance d sees two images: one above and one below the cosmic string as shown in Fig. 6. If the deficit angle is sufficiently close to -2π then an extremal can make several turns around the cosmic string. If the maximal number of rotations for which the inequality (27) is satisfied equals M then the observer sees $2(1+M)$ images: two images caused by the light rays which do not make a rotation before reaching the observer, two images because of the extremals making one rotation, and so on up to M rotations. In Fig. 6(ii) we show a star with four images for $\theta = -3/4$. For this deficit angle any extremal makes one full rotation around the string but two of them reach the observer before making a turn as shown in the picture. Light making an additional rotation reaches an observer later and produces a time delay.

5 Extremals for N wedge dislocations

Let us consider an arbitrary number N of parallel wedge dislocations, characterized by deficit angles θ_n , $n = 1, \dots, N$. The corresponding two-dimensional metric dl^2 in complex coordinates $z = x + iy$ has the form [10]

$$dl^2 = dzd\bar{z} \prod_n [(z - z_n)(\bar{z} - \bar{z}_n)]^{\theta_n}. \quad (31)$$

Here a bar denotes complex conjugation. Dislocations intersect the x, y plane in the points z_n . Direct integration of the corresponding equations for extremals is sophisticated in this coordinate system because in general there is no Killing vector field in the x, y plane. Even in the case of one edge dislocation (the dipole of two wedge dislocations) the problem requires numerical analysis if the metric is first expanded at large distances and then extremals are found [24]. However, the problem becomes almost trivial if one does not expand the metric and note that there is a coordinate system where the metric becomes Euclidean. In complex coordinates denoted by w it has the Euclidean form

$$dl^2 = dwd\bar{w}, \quad (32)$$

where

$$w = u + iv = e^{i\alpha} \int^z d\zeta \prod_n (\zeta - z_n)^{\theta_n} + C. \quad (33)$$

Here α and C are arbitrary real and complex numbers. The contour of integration should not cross and contain closed loops around points z_n . We discuss this integral in detail in Section 6 in several simple cases. If all dislocations go through the x -axis, $\text{Im}z_n = 0$, then this function is called the Christoffel–Schwarz integral (see,

for example, [34]) and is well known in complex analysis. It conformally maps the upper half plane $z > 0$ onto the polygon with one vertex lying at infinity and other vertices at points w_n . Each point z_n is mapped into the vertex w_n with the inner angle $\pi(1+\theta_n)$. In a general case when $\text{Im}z_n \neq 0$ for some dislocations the conformal map becomes more involved.

The integral (33) yields the solution to the Hamilton–Jacobi equation (8)

$$S = \sqrt{2E} \sqrt{(w-c)(\bar{w}-\bar{c})} - Et, \quad c = a + ib = \text{const.}$$

For the Euclidean metric (32) extremals are straight lines,

$$(u-a) \sin \gamma = (v-b) \cos \gamma, \quad (34)$$

or

$$(w-c)e^{-i\gamma} = (\bar{w}-\bar{c})e^{i\gamma} \quad (35)$$

going through a point (a, b) at an angle γ . Scattering of a phonon in real crystal occurs in the original Cartesian coordinates x^μ . Therefore equation (34) has to be written in the original system. This cannot be done for arbitrary distribution of defects because the integral (33) cannot be taken in a general case. To describe scattering of phonons one needs only asymptotics at large distances $|z| \gg |z_n|$. In the following sections we analyze the scattering up to the quadrupole expansion. It is characterized by three global parameters of a distribution.

The total deficit angle (or the charge) normalized on 2π is

$$\Theta = \sum_{n=1}^N \theta_n. \quad (36)$$

We assume that $\Theta > -1$ for the physical reason because one cannot withdraw more than the whole media. The total Burgers vector (the dipole momentum) and the quadrupole momentum normalized on 2π are

$$B = \sum_{n=1}^N \theta_n z_n, \quad (37)$$

$$M = \frac{1}{2} \sum_{n,k=1}^N (\theta_n \theta_k - \theta_n \delta_{nk}) z_n z_k = \frac{1}{2} B^2 - \frac{1}{2} \sum_n \theta_n z_n^2. \quad (38)$$

In this definition the Burgers vector and the quadrupole momentum should be considered as complex numbers. In the next section we define the Burgers vector as a vector. It has the same absolute value as B but differs from the vector joining the origin of the coordinate system with the point B in the complex plane.

The integral (33) has different asymptotics depending on the total deficit angle. We write down the first three terms for different values of Θ .

$$w \approx e^{i\alpha} \left(\frac{1}{\Theta+1} z^{\Theta+1} - \frac{B}{\Theta} z^\Theta + \frac{M}{\Theta-1} z^{\Theta-1} \right) + C, \quad \Theta \neq 0, 1, \quad (39)$$

$$w \approx e^{i\alpha} \left(z - B \ln z - \frac{M}{z} \right) + C, \quad \Theta = 0, \quad (40)$$

$$w \approx e^{i\alpha} \left(\frac{1}{2} z^2 - Bz + M \ln z \right) + C, \quad \Theta = 1. \quad (41)$$

In the case $\Theta = 0$ no wedge of media is added or removed. The values $\Theta = 1, 2, \dots$ determine the position of \ln -term in the expansion of $w(z)$. The quadrupole term is logarithmic for $\Theta = 1$.

Expansions (39)–(41) show that any extremal going to infinity in the z -plane goes also to infinity in the w -plane. In the latter case extremals are obviously complete, and thus they are complete in the z -plane. If an extremal does not go to infinity then it is also complete because it is either closed or it can be continued to infinite value of the canonical parameter within a finite domain. Note that we have only conical singularities and extremals can be naturally continued through them.

If the total angle $\Theta \neq 0$ then the behavior at large distances is characterized by the first term in equation (39) describing single wedge dislocation discussed in the previous section. Therefore we consider the dipole and quadrupole approximation in the following sections.

6 Conformal maps and dislocations

The integral (33) provides a conformal map between a plane with arbitrary number of conical singularities corresponding to wedge dislocations (z -plane) and a Riemannian surface (covered by w -coordinates) with the Euclidean metric. This map has a clear physical interpretation corresponding to a defect creation. One starts with the Euclidean plane, then cuts or adds parts of the plane making a Riemannian surface with boundaries. Then the boundaries are glued together. The gluing process is uniquely defined by the conformal map. The points on a boundary are considered as the same if they correspond to the same point on the cut in the z -plane. Below we consider several examples of conformal maps defining the defects considered in the present paper.

The Christoffel–Schwarz integral depends on two constants. We suppose that the point z_1 always coincides with the origin of the coordinate system in the z -plane, and no point z_n , $n = 2, 3, \dots$, lies on the negative half of the real axis. Then the constants may be chosen in such a way that the point w_1 coincides with the origin in the w -plane and negative part of x -axis is mapped onto negative part of the u -axis.

The simplest example of the Christoffel–Schwarz map (33) is provided by the wedge dislocation discussed in Section 3. In this case we have only one dislocation core located in the origin of the coordinate system

$$z_1 = 0, \quad \theta_1 = \theta.$$

The corresponding conformal map is given by the function

$$w = \frac{e^{-i\pi\theta}}{1 + \theta} z^{1+\theta}, \quad (42)$$

and is shown in Fig. 7. The Christoffel–Schwarz integral maps the upper half plane into the polygon with two vertices. One vertex is located at infinity while the other coincides with the origin $w_1 = 0$ and has inner angle $\pi(1 + \theta)$. The whole z -plane

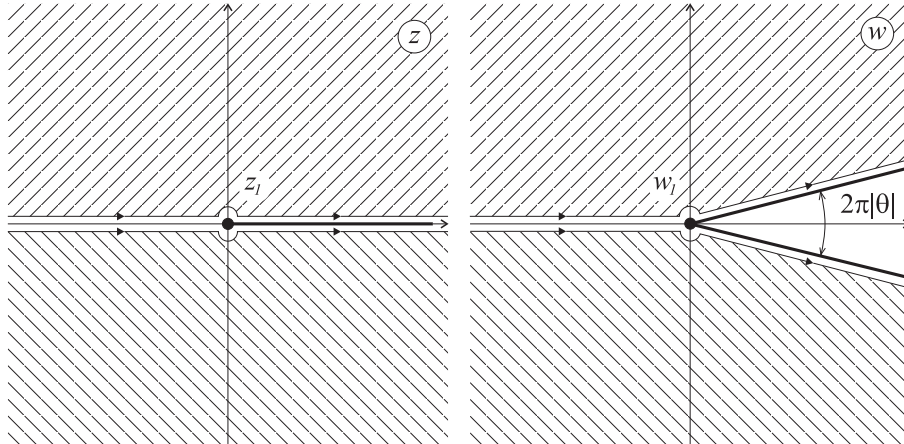


Figure 7: The Christoffel–Schwarz conformal map for a wedge dislocation.

with a cut along the positive half of the real axis is mapped onto the w -plane with the wedge of deficit angle $2\pi\theta$ removed or added to the plane for $-1 < \theta < 0$ or $0 < \theta$, respectively. This conformal map reflects the process of the creation of a wedge dislocation. One takes an infinite elastic media without a defect, cuts out the wedge $2\pi|\theta|$ for $-1 < \theta < 0$, and identifies the points corresponding to the same point on the cut in the z -plane. For $0 < \theta$ one has to cut the w -plane, move apart the sides, and insert the wedge of a media without stresses.

The dipole of two wedge dislocations is called an edge dislocation and is characterized by a constant Burgers vector \vec{B} to be defined later. To construct the conformal map we choose the following locations and angles of the wedge dislocations

$$\begin{aligned} z_1 &= 0, & \theta_1 &= -\theta, \\ z_2 &= h, & \theta_2 &= \theta. \end{aligned} \quad (43)$$

We assume that $0 < \theta < 1$. Then the Christoffel–Schwarz integral (33) takes the form

$$w = \int_0^z d\zeta \left(\frac{\zeta - h}{\zeta} \right)^\theta. \quad (44)$$

Here the constants are chosen in such a way that $w_1(z_1) = 0$. Location of the second vertex in the upper half plain (see Fig. 8) is expressed in terms of the gamma-functions

$$w_2 = \int_0^h d\zeta \left(\frac{\zeta - h}{\zeta} \right)^\theta = h e^{i\pi\theta} \int_0^1 dx \left(\frac{1-x}{x} \right)^\theta = h e^{i\pi\theta} \Gamma(1-\theta)\Gamma(1+\theta). \quad (45)$$

In Fig. 8 we show the conformal map for $1/2 < \theta < 1$. The z -plane has a cut along the positive part of the real axis. The upper half plane is mapped onto the triangle in the upper half of the w -plain with one vertex lying at infinity. The lower half of the z -plain is mapped symmetrically. The whole z -plain with the cut is mapped

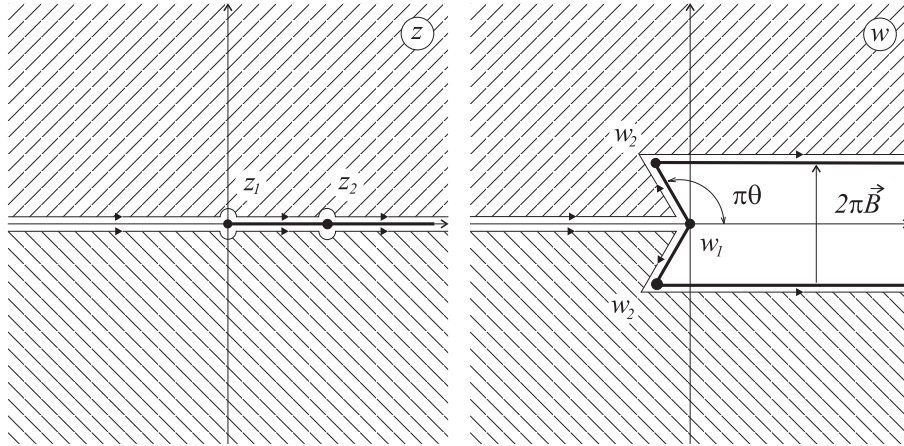


Figure 8: The Christoffel–Schwarz conformal map for a dipole of two wedge dislocations representing one edge dislocation.

onto the w -plane with the removed strip as shown in the picture. We define the Burgers vector as the vector joining two points w_- and w_+ corresponding to lower and upper shores of the cut in the z -plane. For an edge dislocation for $x > z_2$ it is a constant vector. The absolute value of the normalized vector is

$$2\pi|\vec{B}| = w_+ - w_- = 2\text{Im}w_2. \quad (46)$$

This definition is applicable for arbitrary distribution of wedge dislocations. In a general case the cut may be defined as the line joining the sequence of points z_1, \dots, z_N, ∞ including the infinite point. Of course, the corresponding Burgers vector may not be constant. Using the expression (45) and the property of gamma-functions we get for an edge dislocation

$$2\pi|\vec{B}| = 2h\Gamma(1 - \theta)\Gamma(1 + \theta)\sin(\pi\theta) = 2h\pi\theta.$$

This remarkable result shows that the normalized Burgers vector equals the product $h\theta$. Note that this is an exact result for a dipole of two wedge dislocations, and it coincides with the definition (37) for the distribution (43) used in the large distance expansion of the Christoffel–Schwarz integral.

Let us compare the conformal map for a dipole of wedge dislocations with the conformal map (40) of the pure edge dislocation $\Theta = 0$, and $B \neq 0$

$$w = z - B \ln z + i\pi B, \quad (47)$$

where we have specified the values of the constants. Elementary analysis yields the conformal map shown in Fig. 9. It maps the upper half plane of the z -plane onto the upper half plain of the w -plane with the cut as shown in the picture. The origin of the coordinate system is mapped into the infinite point, $w_1(z_1) = \infty$. This

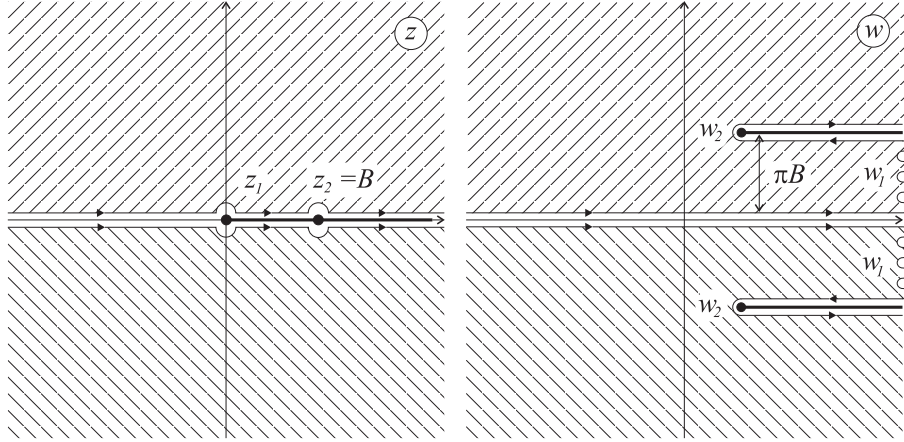


Figure 9: The conformal map in the dipole approximation (an edge dislocation).

conformal map has less clear physical interpretation but is more universal because it does not depend on the details of the distribution at small distances.

The pure quadrupole distribution of wedge dislocations may be organized in the following way

$$\begin{aligned}
 z_1 &= 0, & \theta_1 &= -\theta, \\
 z_2 &= h, & \theta_2 &= \theta, \\
 z_3 &= l, & \theta_3 &= \theta, \\
 z_4 &= l + h, & \theta_4 &= -\theta,
 \end{aligned}$$

where h, l , and θ are constants. For definiteness we assume that $l > h$ and $0 < \theta < 1$. Then only the quadrupole momentum differs from zero

$$\Theta = 0, \quad B = 0, \quad M = \theta lh.$$

The corresponding conformal map is provided by the Christoffel–Schwarz integral

$$w = \int_0^z d\zeta \left[\frac{(\zeta - h)(\zeta - l)}{\zeta(\zeta - l - h)} \right]^\theta. \quad (48)$$

It cannot be taken in elementary functions but may be analyzed qualitatively. The location of the vertices in the upper half of the w -plane is given by the convergent integrals

$$\begin{aligned}
 w_2 &= h e^{i\pi\theta} \int_0^1 dx \left[\frac{(1-x)(p-x)}{x(p+1-x)} \right]^\theta, \\
 w_3 &= w_2 + (l-h) \int_0^1 dx \left[\frac{x(1-x)}{(q+x)(q+1-x)} \right]^\theta, \\
 w_4 &= w_3 + h e^{-i\pi\theta} \int_0^1 dx \left[\frac{(1-x)(p-x)}{x(p+1-x)} \right]^\theta,
 \end{aligned}$$

where

$$p = \frac{l}{h} > 1, \quad q = \frac{h}{l-h} > 1.$$

We see that $\text{Im}w_4 = 0$. The lower half plain is mapped symmetrically. The corresponding conformal map is shown in Fig. 10. This conformal map has evident

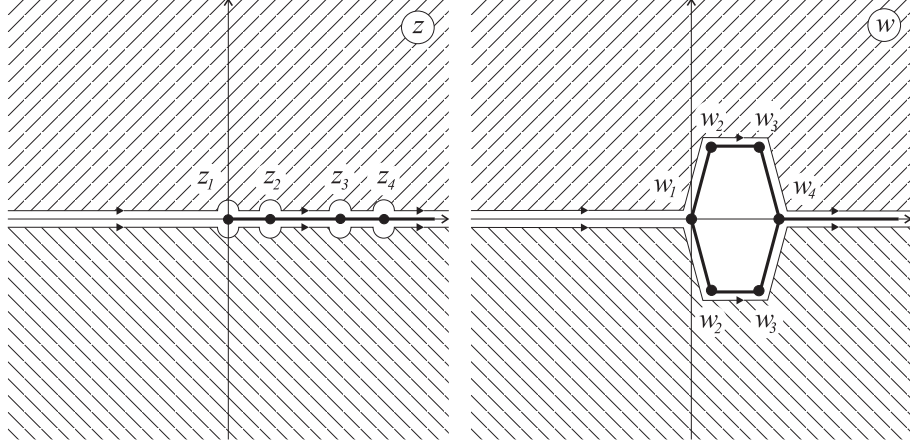


Figure 10: The conformal map for the four wedge dislocations representing the quadrupole source.

physical interpretation. The dislocation is made by withdrawing a hexagonal tube of media.

In the pure quadrupole approximation, $\Theta = 0$, $B = 0$, the conformal map for arbitrary distribution of defects (40) takes the form

$$w = z - \frac{M}{z}, \quad (49)$$

where the constants have been specified. It maps circles into ellipses as shown in Fig. 11. The circles of radius greater than \sqrt{M} are mapped preserving orientation, and the outer part of the z -plain, $|z| > \sqrt{M}$ is mapped onto the whole w -plain with the cut along the imaginary axis. The inner circles are mapped with opposite orientation, and the interior $|z| < 0$ also covers the whole w -plain. We see that the function (49) maps the whole z -plain onto a Riemann surface consisting of two copies of w -plain glued together along the cut. We leave it to the reader to imagine how this conformal map reflects the defect creation.

7 The dipole approximation

If the total deficit angle equals zero, $\Theta = 0$, and $B \neq 0$ then the scattering at large distances is described by the dipole term in (40). The line element corresponding

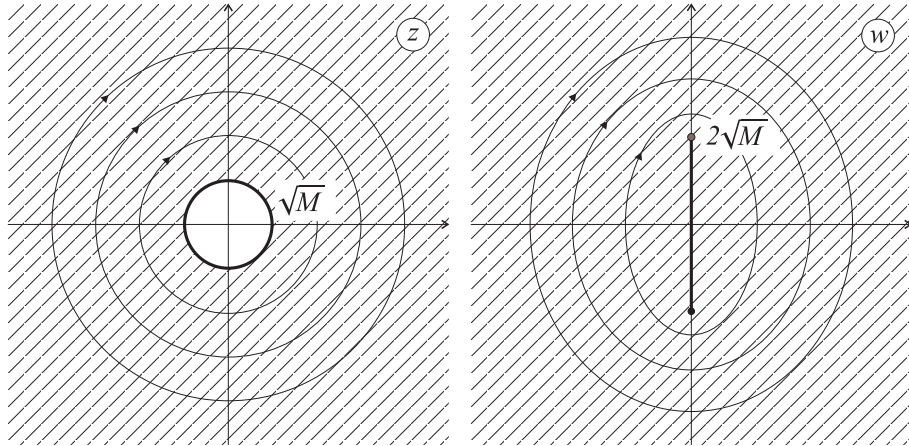


Figure 11: The conformal map in the quadrupole approximation.

to the conformal transformation (47) in polar coordinates is asymptotically flat

$$dl^2 = \left(1 - B \frac{2 \cos \varphi}{r}\right) (dr^2 + r^2 d\varphi^2). \quad (50)$$

The extremals (34) have the form

$$r \sin(\varphi - \gamma) + B(\ln r \sin \gamma + \varphi \cos \gamma) - a \sin \gamma + b \cos \gamma = 0. \quad (51)$$

In the dipole approximation the scattering is characterized by the vector, and trajectories depend on the angle at which extremals go to infinity. We consider two cases. For $\gamma = 0$ the trajectories at infinities are perpendicular to the Burgers vector. In this case equation (51) reduces to

$$\frac{y}{x} = -\tan \frac{y+b}{B},$$

and extremals are parametrized by one arbitrary constant b . In figure 12 extremals are shown for $b = 0$ and $b > 0$, respectively. Extremals for $b < 0$ are obtained from those depicted in Fig. 12 (ii) by the reflection $y \rightarrow -y$. Extremals have asymptotes at infinity shifted by πB . So the net result of the scattering is the shifting of a phonon trajectory defined by the Burgers vector and a time delay. Note the existence of returning trajectories near the dislocation when phonons move from the right. If phonons move from the left there is no backward scattering. It means that an edge dislocation is "invisible" when it is being seen perpendicular to the Burgers vector from the left.

The extremals which are parallel to the Burgers vector at infinity have different behavior and are shown in Fig. 13. They correspond to $\gamma = \pi/2$ and are defined by the equation

$$x^2 + y^2 = \exp\left(2\frac{x+a}{B}\right). \quad (52)$$

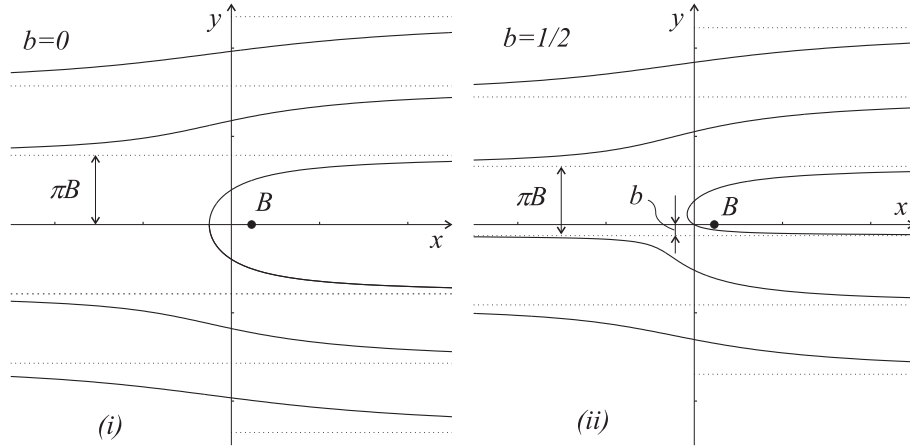


Figure 12: Extremals for the edge dislocation for $b = 0$ (i) and $b = 1/2$ (ii) which are perpendicular to the Burgers vector at infinity. For any $b \neq 0$ the returning extremal goes through the core of dislocation.

In this case they are parametrized by one arbitrary constant a . At infinity the extremals have no asymptotes. This means that even at infinity the observer can feel the dislocation because trajectories are not straight lines. There is also a time delay. For $a = a_0$ where

$$a_0 = B \ln B$$

the extremal has the intersection point at $(B, 0)$. For $a > a_0$ an extremal has one branch. If $a < a_0$ then solution of equation (52) has two branches. One branch starts and ends at infinity while the other is closed and surrounds the dislocation core. In fact this branch may not be closed if the velocity along the x^3 axis is nonzero. In that case it looks like a spiral.

Let us remind the reader that extremals are drawn for the dipole approximation, and therefore one may expect qualitative agreement at large distances from the core of dislocation.

Extremals for an edge dislocation were analyzed numerically in [24]. Qualitative behavior is the same except for the loss of returning trajectories in Fig. 12 and closed trajectories in Fig. 13.

8 The quadrupole approximation

In the quadrupole approximation, $\Theta = 0$, $B = 0$, $M \neq 0$, the conformal map (40) at large distances reduces to

$$w = z - \frac{M}{z}. \tag{53}$$

Without loss of generality we set $\text{Im}M = 0$ and suppose that $M > 0$. To get the scattering for negative M one has to turn the whole picture on the angle π . The

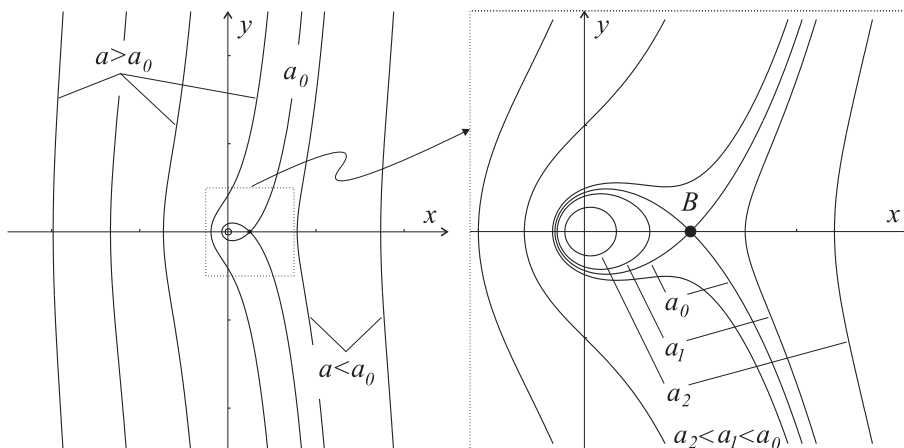


Figure 13: Extremals for an edge dislocation which are parallel to the Burgers vector at infinity. They have no asymptotes. For $a < a_0$ an extremal has two branches.

line element corresponding to the conformal map (53) has the form

$$dl^2 = \left(1 + 2M \frac{\cos(2\varphi)}{r^2} \right) (dr^2 + r^2 d\varphi^2) \quad (54)$$

and goes to the Euclidean line element faster than in the dipole approximation as $r \rightarrow \infty$. In the quadrupole approximation equation (34) for an extremal reduces to

$$r \sin(\varphi - \gamma) + \frac{M}{r} \sin(\varphi + \gamma) - a \sin \gamma + b \cos \gamma = 0. \quad (55)$$

At infinity $r \rightarrow \infty$ this equation coincides with that for a straight line, and therefore any extremal has asymptote. Let us consider two cases. Extremals parallel to the x axis at infinity correspond to $\gamma = 0$ and are defined by the equation

$$x^2 + y^2 = -\frac{My}{y+b}. \quad (56)$$

There is no extremal for $b = 0$. For negative $b < 0$ all extremals lie in the upper half plane and are shown in Fig. 14(i). Extremals for $b > 0$ are obtained from those for $b < 0$ by reflection $y \rightarrow -y$. For $-2\sqrt{M} < b < 0$ an extremal has only one branch going from $x = -\infty$ to $x = +\infty$ and touching the x -axis at the origin of the coordinate system. If $b = -2\sqrt{M}$, then the extremal has the intersection point at $x = 0$, $y = \sqrt{M}$. For $b < -2\sqrt{M}$ an extremal consists of two branches. One infinite branch goes from $x = -\infty$ to $x = +\infty$ and does not touch the x -axis. The other branch is closed and goes through the origin. Any infinite branch has the same asymptote $y = -b$ at both sides as $x \rightarrow \pm\infty$, and the scattering reduces to a time delay.

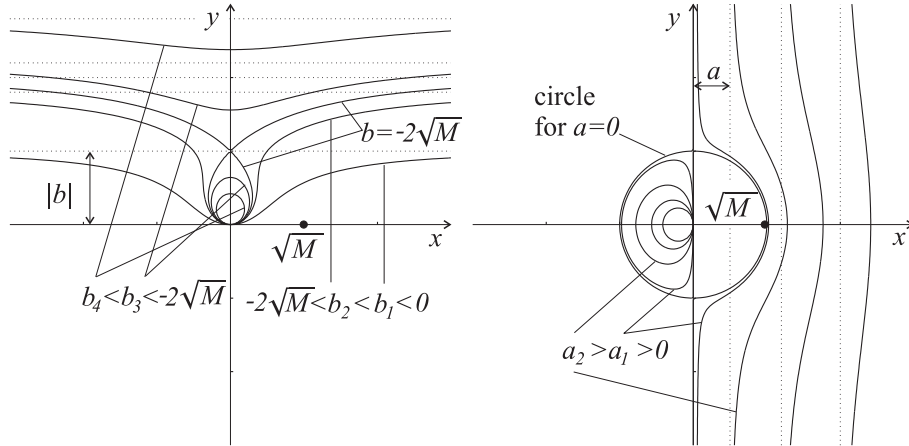


Figure 14: Extremals in the quadrupole approximation which are parallel to x –
(i) and y -axis *(ii)* at infinity. An extremal has two branches for $b < -2\sqrt{M}$ and
arbitrary a .

The extremals parallel to the y axis at infinity correspond to $\gamma = \pi/2$ and are defined by the equation

$$x^2 + y^2 = \frac{Mx}{x - a}.$$

It differs from (56) by the sign in the right hand side and the exchange $x \leftrightarrow y$. Here M is also supposed to be positive. For $a = 0$ the extremal is the circle of radius \sqrt{M} . Extremals with positive $a > 0$ are shown in Fig. 14*(ii)*. Extremals corresponding to negative $a < 0$ are obtained by the reflection $x \rightarrow -x$. Any extremal consists of two branches. One branch is infinite and goes from $y = -\infty$ to $y = +\infty$ with the same asymptote $x = a$. The other branch is closed and located within the circle on the other half of the plane. It goes through the origin. So the scattering reduces only to a time delay.

9 Continuous distribution of defects

One of the main advantages of geometrical description of defects is the possibility to describe continuous distributions of dislocations and disclinations. First, we consider circularly symmetric distribution of wedge dislocations. They are assumed to be uniformly distributed on the disk of radius R with the following density of deficit angles

$$\rho(r) = \begin{cases} q, & r \leq R, \\ 0, & r > R. \end{cases}$$

The normalized total deficit angle for this distribution is

$$\Theta = \frac{1}{2}qR^2.$$

The conformal factor of the corresponding metric

$$g_{\alpha\beta} = e^{2\phi}\delta_{\alpha\beta} \quad (57)$$

satisfies the three-dimensional Einstein equations which in the considered case reduce to the Poisson equation [10]

$$\Delta\phi = -\rho(r)$$

and is defined by the integral

$$\phi(r) = \frac{1}{2\pi} \int d\vec{s} \rho(\vec{s}) \ln |\vec{s} - \vec{r}|.$$

The result is

$$\phi(r) = \begin{cases} \frac{q}{2}R^2 \ln R - \frac{qR^2}{4} + \frac{qr^2}{4}, & r \leq R, \\ \frac{q}{2}R^2 \ln r, & r > R. \end{cases} \quad (58)$$

Outside the dislocations the line element has the form

$$dl^2 = r^{qR^2} (dr^2 + r^2 d\varphi^2).$$

This means that the distribution of wedge dislocations as seen from the outside is the same as for one wedge dislocation (11) with the deficit angle Θ . Therefore trajectories of phonons at large distances are the same as for a single wedge dislocation. This is the result one would not expect because Einstein equations are nonlinear, and, in general, there is no superposition principle. Note that metric (57) with the conformal factor (58) is the exact solution to the Einstein equations.

Now we consider the continuous distribution of edge dislocations characterized by the density of the normalized Burgers vector $\vec{\beta}(\vec{r}) = (\beta_x, \beta_y)$. It is assumed to be directed along the x -axis, $\beta_y = 0$, and uniformly distributed on the disk of radius R

$$\beta_x = \begin{cases} \beta, & r \leq R, \\ 0, & r > R. \end{cases}$$

In this case the Einstein equations also reduce to the Poisson equation for the conformal factor

$$\Delta\phi = 2\pi(\vec{\nabla} \cdot \vec{\beta}).$$

Its solution has the form

$$\phi = \begin{cases} \frac{\beta r \cos \varphi}{2}, & r < R, \\ \frac{\beta R^2 \cos \varphi}{2r}, & r > R. \end{cases} \quad (59)$$

At large distances, $r \gg R$, the space is described by the line element (50) with

$$B = \beta\pi R^2, \tag{60}$$

and is asymptotically flat. We see that at large distances the continuous distribution of edge dislocations behaves like one edge dislocation with the total Burgers vector (60). The superposition principle is valid only for the main term in the line element. There are further corrections which distinguish one edge dislocation from the continuously distributed ones. The first correction may be easily obtained in complex coordinates. The conformal factor (59) outside the distribution yields the line element

$$dl^2 = \exp\left(-B\left(\frac{1}{z} + \frac{1}{\bar{z}}\right)\right) dzd\bar{z}.$$

It may be written in flat form $dl^2 = dwd\bar{w}$, where

$$w = \int^z d\zeta \exp\left(-\frac{B}{\zeta}\right) \simeq z - B \ln z - \frac{B^2}{2z}.$$

This expansion yields the quadrupole correction, $M = B^2/2$, to the continuous distribution of edge dislocations.

10 Conclusion

In the geometrical theory of defects an elastic media is assumed to be a manifold equipped with a Riemann–Cartan geometry, curvature and torsion tensors describing the surface densities of disclinations and dislocations, respectively. When disclinations are absent then curvature is equal to zero and the corresponding $SO(3)$ -connection can be locally gauged away. Then geometry is entirely defined by the triad satisfying the three-dimensional Einstein equations. For a given triad (or a metric) one has two choices: either to consider a manifold as a Riemannian one with Christoffel’s symbols as a connection and nontrivial curvature or to introduce a torsion in such a way that curvature corresponding to the metrical connection is identically zero (a manifold with absolute parallelism if one excludes paths around the singularities). In the last case the manifold has nontrivial torsion defined by the triad only. In this sense three-dimensional gravity and geometric theory of dislocations differ but the solution to one problem yields immediately the solution to the other and vice versa. That is a solution to the three-dimensional Einstein equations may be always interpreted as some distribution of defects in elastic media. The correspondence between the notions is as follows:

spinless point particle	=	wedge dislocation
point particle with spin	=	screw dislocation
static point particles	=	parallel dislocations
moving point particles	=	non parallel dislocations.

Recently solutions for moving particles with and without spins were found in three-dimensional gravity [35-38]. It means that the Euclidean version of this solution describes an arbitrary number of arbitrary oriented wedge and screw dislocations. This problem is so complicated in the framework of ordinary elasticity theory that it can hardly be solved. At the same time it can be solved in the framework of the geometric theory of defects.

Another advantage of the theory of defects concerns the propagation of elastic waves in the presence of defects considered in the paper. We are not aware how to formulate this problem unambiguously even for a single dislocation in the framework of elasticity theory. At the same time the geometrical approach adopted in the present paper provides an almost standard and simple answer: the perturbations propagate along extremals for a metric describing given distribution of dislocations. In this way we have found trajectories of phonons. Their behavior is quite different from that in the potential motion of point particles. We hope that this non-potential motion of phonons in the presence of defects may be confirmed or refuted experimentally in the future. Maybe elastic media provides a much better experimental field for testing gravity models.

In the present paper we have shown that a star located behind a cosmic string may produce any even number of images. The number of images is larger when the deficit angle is closer to -2π . Analogous behavior of extremals is encountered also in general relativity already for the Schwarzschild solution [32]. This effect leads to the appearance of multiple images of a star located behind the singularity and changes the usual description of gravitational lensing. If the singularity is strong enough then an observer sees not two but a large even number of images of a star. There is a wide field of speculations about what we really see in the sky.

This work is supported by the Russian Foundation for Basic Research, Grants RFBR-96-010-0312 and RFBR-96-15-96131.

References

- [1] É. Cartan. *Comptes Rendus de l'Academie des Sciences (Paris)*, 174 (1922), 593.
- [2] É. Cartan. *On Manifolds with an Affine Connection and the Theory of General Relativity*. Bibliopolis, Naples, 1986.
- [3] K. Kondo. On the geometrical and physical foundations of the theory of yielding. In *Proc. 2nd Japan Nat. Congr. Applied Mechanics*, page 41, Tokyo, 1952.
- [4] B. A. Bilby, R. Bullough, and E. Smith. *Proc. Roy. Soc. London*, A231 (1955), 263.
- [5] E. Kröner. Continuum theory of defects. In R. Balian et al., editor, *Less Houches, Session XXXV, 1980 – Physics of Defects*, pages 282–315. North-Holland Publishing Company, 1981.

- [6] A. Kadić and D. G. B. Edelen. *A gauge theory of dislocations and disclinations*. Springer–Verlag, Berlin – Heidelberg, 1983.
- [7] H. Kleinert. *Gauge fields in condensed matter*, volume 2. World Scientific, Singapore, 1990.
- [8] I. E. Dzyaloshinskii and G. E. Volovik. On the concept of local invariance in the theory of spin glasses. *J. Physique*, 39 (1978), 693.
- [9] E. Cosserat and F. Cosserat. *Théorie des corps déformables*. Hermann, Paris, 1909.
- [10] M. O. Katanaev and I. V. Volovich. Theory of defects in solids and three-dimensional gravity. *Ann. Phys.* 216 (1992), 1.
- [11] J. Madore. The Geometry of Defects. *Preprint LPTHE, Orsay*, (1996), 5 pp.
- [12] F. W. Hehl, J. D. McCrea, E. W. Mielke, and Y. Ne’eman. Metric-affine gauge theory of gravity: Field equations, Noether identities, world spinors, and breaking of dilaton invariance. *Phys. Rep.* 258 (1995), 1.
- [13] A. Staruszkiewicz. Gravitational theory in three-dimensional space. *Acta Phys. Polon.* 24 (1963), 735.
- [14] G. Clement. Field–theoretic particles in two space dimensions. *Nucl. Phys. B* 114 (1976), 437.
- [15] S. Deser, R. Jackiw, and G. ’t Hooft. Three-dimensional Einstein gravity: Dynamics of flat space. *Ann. Phys.* 152 (1984), 220.
- [16] A. Holz. Geometry and action of arrays of disclinations in crystals and relation to (2+1)-dimensional gravitation. *Class. Quantum Grav.* 5 (1988), 1259.
- [17] A. Holz. Topological properties of linked disclinations and dislocations in solid continua. *J. Phys. A* 25 (1992), L1.
- [18] C. Kohler. Point particles in 2+1-dimensional gravity as defects in solid continua. *Class. Quantum Grav.* 12 (1995), L11.
- [19] C. Kohler. Line defects in solid continua and point particles in (2 + 1)-dimensional gravity. *Class. Quantum Grav.* 12 (1995), 2977.
- [20] R. A. Puntigam and H. H. Soleng. Volterra distortions, spinning strings, and cosmic defects. *Class. Quantum Grav.* 14 (1997), 1129.
- [21] C. Furtado and F. Moraes. On the binding of electrons and holes to disclinations. *Phys. Lett.* A188 (1994), 394.

- [22] C. Furtado, B. G. C. da Cunha, F. Moraes, E. R. Bezerra de Mello, and V. B. Bezzerra. Landau levels in the presence of disclinations. *Phys. Lett.* A195 (1994), 90.
- [23] F. Moraes. Enhancement of the magnetic moment of the electron due to a topological defect. *Mod. Phys. Lett.* A10 (1995), 2335.
- [24] F. Moraes. Geodesics around a dislocation. *Phys. Lett.* A214 (1996), 189.
- [25] A. de Padua, F. Parisio-Filho, and F. Moraes. Geodesics Around Line Defects in Elastic Solids. *Phys. Lett.* A238 (1998), 153.
- [26] A. P. Balachandran, V. John, A. Momen, and F. Moraes. Anomalous defects and their quantized transverse conductivities. *Int. J. Mod. Phys.* A13 (1998), 841.
- [27] L. D. Landau and E. M. Lifshitz. *The Classical Theory of Fields*. Pergamon, New York, second edition, 1962.
- [28] H. Kleinert. Non-abelian bosonization as a nonholonomic transformation from a flat to a curved field space. *Ann. Phys.* 253 (1997), 121.
- [29] A. Vilenkin and E. Shellard. *Cosmic Strings and Other Topological Defects*. Cambridge University Press, Cambridge, 1994.
- [30] M. B. Hindmarsh and T. W. B. Kibble. Cosmic strings. *Rep. Prog. Phys.* 58 (1995), 477.
- [31] G. E. Volovik. Simulation of Quantum Field Theory and Gravity in Superfluid He-3, *cond-mat/9706172*. (1997) 6 pp.
- [32] S. Chandrasekhar. *The mathematical theory of black holes*, volume 1,2. Clarendon Press, Oxford, 1983.
- [33] A. Vilenkin. Gravitational field of vacuum domain walls and strings. *Phys. Rev.* D23 (1981), 852.
- [34] M. A. Evgrafov. *Analytic Functions*. Nauka, Moscow, third edition, 1991. [In Russian].
- [35] A. Bellini, M. Ciafaloni, and P. Valtancoli. Non-perturbative Particle Dynamics In $(2 + 1)$ -Gravity, *Phys. Lett.* B357 (1995), 532.
- [36] A. Bellini, M. Ciafaloni, and P. Valtancoli. $(2 + 1)$ -gravity with moving particles in an instantaneous gauge. *Nucl. Phys.* B454 (1995), 449.
- [37] A. Bellini, M. Ciafaloni, and P. Valtancoli. Solving the N -body problem in $(2 + 1)$ -gravity. *Nucl. Phys.* B462 (1996), 453.
- [38] M. Ciafaloni and P. Valtancoli. $(2 + 1)$ -gravity solutions with spinning particles. *Class. Quantum Grav.* 14 (1997), 955.